

Study of surface plasmon resonance with zirconium oxide multilayer coatings of silver and gold films: reflection polarization modes and sensitivity

H. H. Sánchez Hernández

*Universidad del Papaloapan, Instituto de Ingeniería, Loma Bonita, Oaxaca, México,
e-mail: hehusan@unpa.edu.mx*

J. M. Pérez Abarca

*Universidad del Papaloapan, Instituto de Ingeniería, Loma Bonita, Oaxaca, México,
e-mail: jperez@unpa.edu.mx*

E. Sánchez Soto

*Universidad Tecnológica de la Mixteca, Instituto de Computación, Huajuapán de León, Oaxaca, México,
e-mail: esanchez@mixteco.utm.mx*

Received 5 June 2023; accepted 27 September 2023

We propose a surface plasmon resonance (SPR) sensor based on multilayer films with silver (Ag) and gold (Au) interfaces coated with a thin layer of zirconium oxide (ZrO_2) in Kretschmann configuration. A dielectric layer of ZrO_2 acts as the prism coating and the second layer is deposited after the metal film in the dielectric/metal/dielectric (DMD) system. In order to achieve the best design for the sensor, the dependence of the sensitivity on the angle of incidence and the thickness of the alternating layer is comprehensively explored. The polarization change results are shown with the angles Ψ and Δ which are the traditional ellipsometry measurement angles of the optical properties of the DMD system. The advantage of Ag/ ZrO_2 multilayers over Au and Au/ ZrO_2 for SPR refractive index detection in terms of sensitivity, as well as the Ag/ ZrO_2 interface offers the possibility of studies with promising features for SPR users to generalize this type of interface. The proposed DMD sensor is expected to find application in biochemical sensing due to its resolution.

Keywords: Surface plasmon resonance; silver; gold; dielectric/metal/dielectric.

DOI: <https://doi.org/10.31349/RevMexFis.70.021301>

1. Introduction

Refractive index (IR) sensing is important for biological and chemical applications, many recent works have undertaken the manufacturing and development of biosensors using various sensing methods [1]. Surface plasmon resonance (SPR) is one of them [2, 3]. This method investigates a wide range of different suspected interactions with a variety of biomolecules in real-time without labelling [4]. The surface plasmon (SP) is a charge density oscillation that occurs at the interface between a noble metal, such as gold (Au) or silver (Ag) and a dielectric. So, when there is a change in the refractive index of the dielectric medium, the SP dispersion relation is altered. The change in refractive index alters the characteristics of the light wave coupled to the SP and ultimately changes the resonance conditions. Optical excitation of the plasmon can be achieved through a coupler (prism, grating, planar or cylindrical waveguide) coated with a suitable thin metallic film, or by direct interaction of light with nanoparticles [5]. The bulky SPR sensors can be attributed to the successful exploitation of the phenomenon in commercial and industrial applications. The recognised intrinsic capabilities of the technique, the versatility and adaptability of the configuration to customer needs and the possibility of multi-parametric sensing have contributed to its success. When a dielectric layer is incorporated on the metal film, a waveguide structure is created that supports both plasmonic and conven-

tional wave modes [6]. Because of the narrower waveguide resonances compared to SPR, this structure overcomes some of the limitations of plasmonic sensors. However, to obtain the highest sensor sensitivity, nanometre-sized holes must be created in the waveguide to maximise the superposition of the zero-order waveguide mode and the material to be sensed. We believe that a study of a comprehensive range of surface plasmon resonance spectral data on noble metals in various parameter spaces is an important prelude to the future application of more sophisticated spectroscopic techniques for the experimental determination of fundamental surface plasmon properties. This paper is to consider a modified type of plasmonic waveguide sensor [7] with the noble metals Ag and Au having a dielectric-metal-dielectric-analyte (DMDA) [8] structure that supports conventional TM (transverse magnetic) plasmonic waveguide modes. The DMDA structure is specially designed to further decrease propagation losses and enhance the evanescent field, thus increasing the resolution and sensitivity of the sensor.

2. Methods

We consider the DMDA structure composed of a BK7 glass prism of refractive index ($n_1 = 1.515$), for the Ag film: $d = 55.11$ nm, $\epsilon_{Au} = -18.631 + 0.4425i$ and for the Au film: $d = 49.55$ nm, $\epsilon_{Au} = -12.998 + 1.033i$ [9]; both films

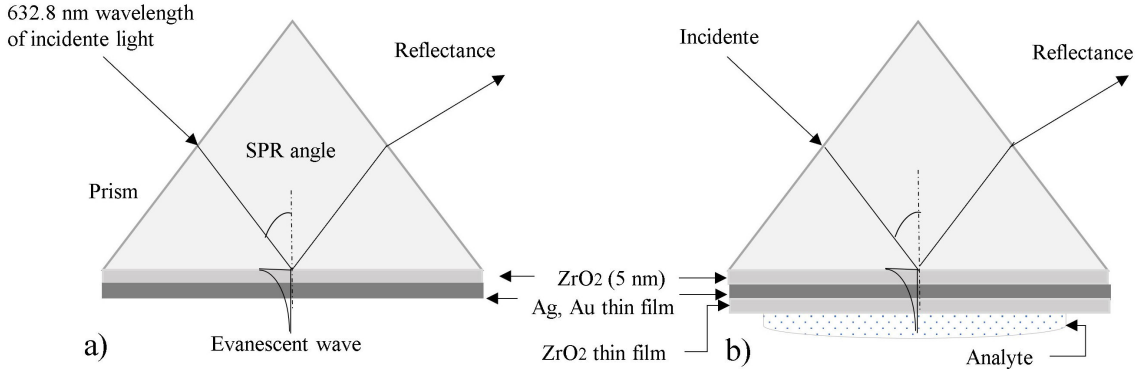


FIGURE 1. Structure of the multilayer sensor consisting of the prism, ZrO_2 , Ag/Au, ZrO_2 and analyte.

with a high refractive index layer [Fig. 1b)]. As the high-index (H) layer, we consider ZrO_2 ($n = 2.151$) [10] at wavelength $\lambda = 632.8$ nm, the sensing medium (analyte) used on the transmission side depends drastically on the refractive index $n_s = 1.333$ [11], since the mode attenuation of the surface plasmon wave (SPW) depends on the refractive index of the analyte. The core operation of this structure is based on the total internal reflection phenomenon. Calculations are made with the S-matrix method [12]. We establish the optimum layer thicknesses, which provide the maximum of the field enhancement (see Fig. 2) for the last dielectric layer.

In order to observe the excitation of the surface plasmon polarization (SPP) in the Kretschmann configuration, polarized light ($\lambda = 632.8$ nm) was incident on the DMDA layer at the prism side in the simulation, shown in Fig. 1, corresponding to the reflection behaviour. In p -polarized light, surface plasmons are excited at the metal-dielectric interface and resonance decay appears in the reflection spectrum. The simulation of this process was performed to evaluate the reflectance (R_p) using the multilayer (N -layer) model described in reference [13]. This model defines a layered medium as a stack of homogeneous thin films (N -layer) of thickness d_k , permeability μ_k , the dielectric constant ϵ_k and refractive index n_k are related according to $n_k = \sqrt{\epsilon_k}$ for each layer along the Z -direction. Furthermore, this model assumes that all layers are uniform, isotropic and non-magnetic, with the tangential components of the electric and magnetic fields at the first boundary $Z = Z_1 = 0$ being related to those at the final boundary $Z = Z_{N-1}$ by:

$$\begin{bmatrix} U_1 \\ V_1 \end{bmatrix} = M \begin{bmatrix} U_{N-1} \\ V_{N-1} \end{bmatrix}. \quad (1)$$

In Eq. (1) (U_1 and V_1) and (U_{N-1} and V_{N-1}) are tangential components of the electric (magnetic) field at the boundary of the first and ($N - 1$)-th layer, respectively. M is known as the characteristic matrix of the combined structure, and is mathematically represented as follows:

$$M = \prod_{k=2}^{N-1} M_k = \prod_{k=2}^{N-1} \begin{bmatrix} \cos \beta_k & -i \sin \beta_k / q_k \\ -i q_k \sin \beta_k & \cos \beta_k \end{bmatrix} \quad (2)$$

with

$$\beta_k = \frac{2\pi d_k}{\lambda} (\epsilon_k - n_1^2 \sin^2 \theta_1)^{1/2}, \quad (3)$$

where $n_1 = \sqrt{\epsilon_1}$ represents the refractive index (IR) in the incident medium (prism), λ and θ_1 are the wavelength of the polarized laser beam p and the incident angle measured relative to the normal at the prism-metal layer interface, respectively, β_k is the phase change found at the interface in the layer k_{th} and d is thickness of the layer k . However, q_k is the effective refractive index at the medium, analyte or dielectric, film and is given by:

$$q_k = \begin{cases} n_k / \cos \theta_k & p\text{-polarization} \\ n_k \cos \theta_k & s\text{-polarization} \end{cases} \quad (4)$$

So it depends on whether the incident light is polarized (parallel- p or perpendicular- s) about the incident plane. Finally, the amplitude of reflected wave (r_p) and R_p are given by:

$$r_{p,s} = \frac{(M_{11} + M_{12}q_k)q_1 - (M_{21} + M_{22}q_k)}{(M_{11} + M_{12}q_k)q_1 + (M_{21} + M_{22}q_k)}, \quad (5)$$

$$R_p = |r_p|^2 \quad (6)$$

In order to examine the amplitude and phase changes of the obliquely reflected and transmitted wave within the film, the complex amplitude (r_p parallel and r_s perpendicular) is reflected obliquely and can be written in terms of their values and angles, as follows [14]:

$$r_p = \rho_p e^{i\phi_p}, \quad (7)$$

$$r_s = \rho_s e^{i\phi_s}, \quad (8)$$

ρ_p and ρ_s are the amplitude attenuations of the wave, ϕ_p and ϕ_s represent the electromagnetic wave phases for the parallel p and s perpendicular components. The Kretschmann configuration also provides a better signal-to-noise ratio, which allows the surface plasmons to penetrate the sensing medium for high interactions with the analyte, in general, Eq. (5) represents two polarization states (p and s). A polarization change occurs at the reflection site because of the difference

in attenuation of amplitude and phase shift experienced by the p and s components. The relationship between incident and reflected polarization is represented as follows:

$$\rho = \frac{r_p}{r_s}. \quad (9)$$

The polarization change after reflection from a surface is represented by a complex reflection coefficient:

$$\rho = \tan(\Psi)e^{-i\Delta} \quad (10)$$

so

$$\tan(\Psi) = \frac{\rho_p}{\rho_s}, \quad \Delta = \phi_p - \phi_s \quad (11)$$

The right-hand side of the Eq. (10) is represented as a function $f(n; k; d)$. Applying the ellipsometric, which is a metrology technique that measures a polarization state upon light reflection on a sample surface and is able to determine a film thickness non-destructively with a high accuracy of nanometers and is widely used to investigate the properties of a surface and the films that covers it, with this technique the angles Ψ and Δ are obtained using ellipsometric measurements of optical properties of a polyphase system, that is, the refractive index of the medium, dielectric, film, dielectric and analyte are n_1, n_2, n_3, n_4 and n_5 respectively, the thickness of the metal film d_2 , dielectric thickness d_1 and d_3 for given values in the wavelength emitted beam and incidence angle θ_k in the medium. The equation is written as follows:

$$\rho = f(n_1, n_2, n_3, n_4, n_5, \lambda, d_1, d_2, d_3, \theta_k). \quad (12)$$

The above equation can be divided into two equations for Ψ and Δ , thus:

$$\Psi = \tan^{-1} |f(n_1, n_2, n_3, n_4, n_5, \lambda, d_1, d_2, d_3, \theta_k)|, \quad (13)$$

$$\Delta = \arg [f(n_1, n_2, n_3, n_4, n_5, \lambda, d_1, d_2, d_3, \theta_k)], \quad (14)$$

where $|\rho|$ and $\arg(\rho)$ are absolute values and argument of the complex value ρ .

3. Results and discussion

Results of a numerical simulation (MATLAB software) on the reflectance of the prism coated with a dielectric film $d_1(\text{ZrO}_2, 5 \text{ nm})$ are shown in Fig. 1a); in which there is a metallic layer $d_2(\text{Ag, Au})$ coated with a dielectric thickness $d_3(\text{ZrO}_2)$, it is assumed that this dielectric thickness is varied in order to obtain the minimum reflectivity observed for TM polarisation, as seen in Fig. 1b). The minimum of the reflectivity for d_3 in the silver film and gold is observed in the plasmon polarised resonance at ($R_{\min(\text{Ag})} = 2.525 \times 10^{-7}$, $\theta_{\text{Ag}} = 49.054^\circ$) and ($R_{\min(\text{Au})} = 7.391 \times 10^{-5}$, $\theta_{\text{Au}} = 47.5247^\circ$). In the absence of analyte, the reflectivity decreases with increasing dielectric thickness, the minimum reflectance is found for a thickness in the silver film of $0.196 \mu\text{m}$ and in gold of $0.186 \mu\text{m}$. Using $\lambda = 632.8 \text{ nm}$ and a prism *BK7* of refractive index $n_p = 1.515$, the optimum thickness of the bottom metal layer *ZrO*₂ for which $d = 5 \text{ nm}$, $\varepsilon_2 = 4.629$ (see Fig. 2), for Ag is ($d = 55.11 \text{ nm}$, $\varepsilon_{\text{Ag}} = -18.631 + 0.4425i$) and for Au is ($d = 49.55 \text{ nm}$, $\varepsilon_{\text{Au}} = -12.998 + 1.033i$) [9]. Observe that the SPR generation is mainly influenced by the thickness of the metals. If the metal layer is very thin, the SPPs will be strongly damped due to the damping of the radiation in the prism. If the metal is very thick, the SPPs can no longer be excited effectively due to absorption in the metal. The advantages of a lower layer of dielectric for silver compared to gold becomes more evident by considering the SPR signals of the silver- and gold-based composite films in general. Figure 3 shows the different values of the refractive indices in the analytes, one can see that the refractive index increases, as the reflectivity decreases, so the minimum reflectivity is observed for the analyte with $n_s = 1.333$, for Ag film ($R_{\min(\text{Ag})} = 7.191 \times 10^{-5}$, $\theta_{\text{Ag}} = 68.397^\circ$) and Au found at ($R_{\min(\text{Ag})} = 6.888 \times 10^{-5}$, $\theta_{\text{Ag}} = 67.092^\circ$).

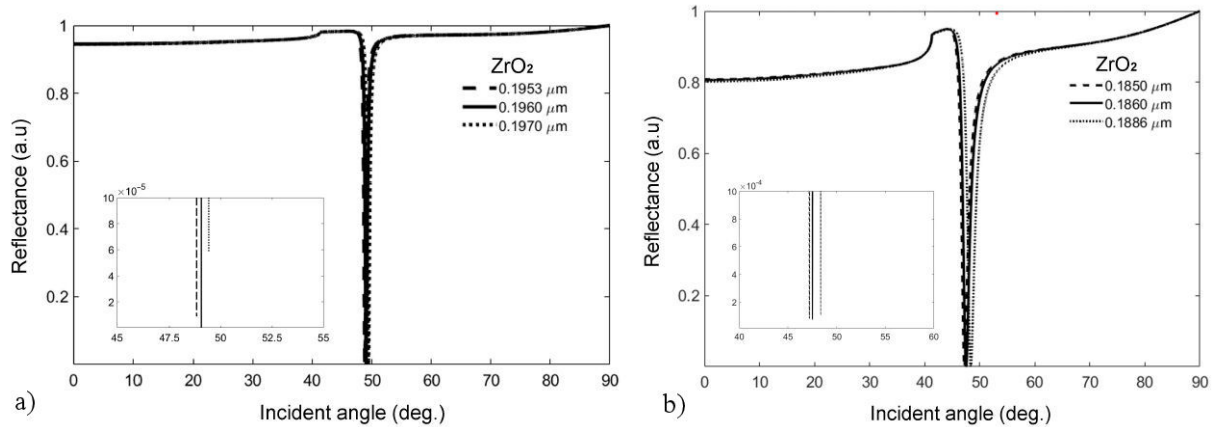


FIGURE 2. a) BK7/ZrO₂(5 nm)/Ag(55.11 nm)/ZrO₂. b) BK7/ZrO₂(5 nm)/Au(49.55 nm)/ZrO₂. Reflectance versus angle of incidence curve with different coating film thicknesses ZrO₂ for Ag a) and Au b).

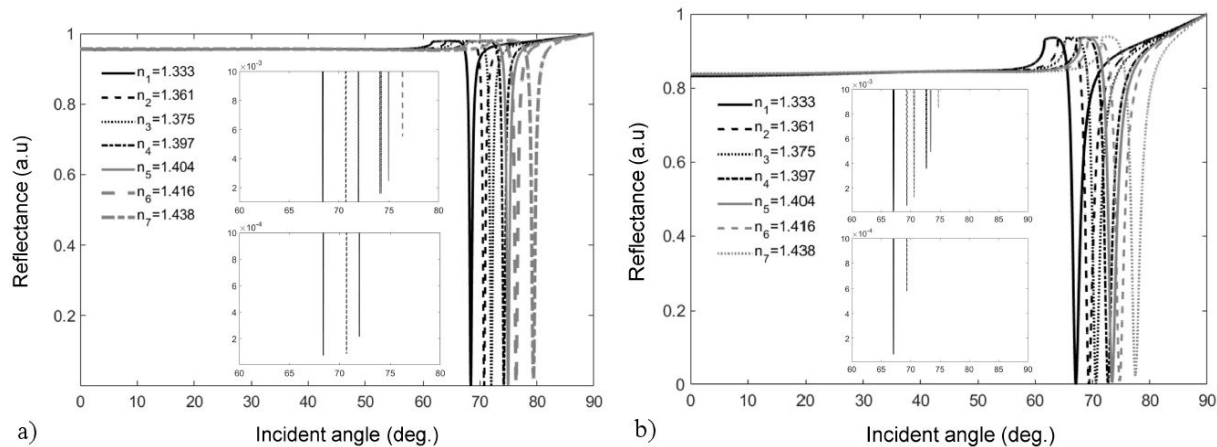


FIGURE 3. a) BK7/ZrO₂(5 nm)/Ag(55.11 nm)/ZrO₂(196 nm)/IR b) BK7/ZrO₂(5 nm)/Au(49.55 nm)/ZrO₂(186 nm)/IR. Reflectance versus angle of incidence curves for the DMD for different refractive indices of analytes.

The angles Ψ and Δ associated with the ellipsometry function (10) are shown Fig. 4, these figures are based on the incidence angle θ_k with values for the film of Ag ($d_{3(\text{ZrO}_2)} = 0.196 \mu\text{m}$) and Au ($d_{3(\text{ZrO}_2)} = 0.186 \mu\text{m}$).

Figures 4a) and 4c) when $\Delta = 0$ or π , light that appears linearly polarised at any azimuthal angle from the incident plane becomes linearly polarised after being reflected by dielectric-metal-dielectric-analyte (DMDA). Hence, it would represent a polarised surface suppression analyser, so when $\Delta = \pi/2$ or $3\pi/2$ the major or minor axes of the polarisation ellipse of the reflected light is linearly polarised for a certain azimuthal angle and is aligned parallel or perpendicular to the incident plane. Figures 4b) and 4d) if $\tan \Psi = 1$ then $R_p = R_s$ and $\rho = e^{i\Delta}$ the DMDA system acts as a reflection retarder. So $\rho = \tan \Psi$ is a minimum or a maximum, this points indicate a given DMDA system closely operates like a suppression polariser s or p .

The SPR measurement signal depends critically on several characteristics of the system, which is related to the refractive index of the metal layer and its thickness. The refractive index of the metal influences the position of the Θ_{SPR} angle and the full width at half maximum (FWHM) in SPR signal and the intensity on the resonance at Θ_{SPR} (ISPR). Gold like silver are light-absorbing interfaces. The parts of the refractive index ($n = n' + in''$) both real and imaginary determine the overall characteristics of the SPR.

For a specific incident wavelength and coupling prism, there is a minimum ISPR and FWHM corresponding to an optimum film thickness. The value of the angle Θ is a function of the refractive indices used in the prism, the metal film, the dielectric layer above and below (dielectric adhesive layer or layers) and also the thicknesses of the metal film. Weak adhesion of metals such as gold and silver on glass implies the use of an adhesion layer such as ZrO₂ prior to the deposition of the metal films, the layer below the metal has a pronounced effect on the SPR profile and is considered thin enough to completely coat the glass substrate and provides a solid adhesion layer for the metal film [15]. The

increase in SPR curves width (FWHM) with growing ZrO₂ thickness demonstrates that the additional layer on the top metal (Ag,Au) must be controlled to a very small thickness. In SPR, a small value of FWHM is advantageous as it shows the ability of the sensor to detect small changes in the refractive index of the analyte [16]. A figure of merit (FOM) was defined by [17] to quantitatively evaluate the refractive index sensitivity of various optical sensors [Eq. (15)], in which m is the slope of the linear regression for the refractive index that depends on $\Theta_{\text{SPR}}/\text{FWHM}$ (Fig. 5). The deeper and narrower the resonance peak, the more accurate is the determination of the Θ_{SPR} position.

$$FOM = \frac{m \text{ (degree } RIU^{-1})}{FWHM \text{ (degree)}} \quad (15)$$

Both parameters are obtained by changing the dielectric medium in contact with the SPR interface. Figure 3 shows the resulting SPR curves when the multilayer interfaces ZrO₂(5 nm)/Ag/ZrO₂(0.196 μm) and ZrO₂(5 nm)/Au/ZrO₂(0.186 μm) are in contact with solutions of increasing refractive indices. The FWHM and ISPR are not strongly influenced by increase in the dielectric constant. Gold-based SPR interfaces on the other hand, show significant changes in the ISPR [Fig. 3b)]. In addition, due to the larger changes of the Θ , the detectable refractive index range decreases with ZrO₂/Au and becomes more pronounced in the ZrO₂/Au/ZrO₂ interface. This is the result of the deeper probing depth of the silver-based SPR interfaces [18]. A stronger evanescent field implies a larger detection region, which is important for monitoring biomolecular interactions of analytes and larger analytes with immobilised species on the surface. Therefore, the FOM is obtained more accurately by determining the linear regression slope m in the graph $\Delta_{\Theta_{\text{SPR}}}/\text{FWHM}$ versus the refractive index of the dielectric medium (Fig. 5). A linear relationship is observed in all cases with a minimum sensitivity of $50.619RIU^{-1}$ for ZrO₂/Au/ZrO₂ and the higher sensitivity of $148.77RIU^{-1}$ for ZrO₂/Ag/ZrO₂.

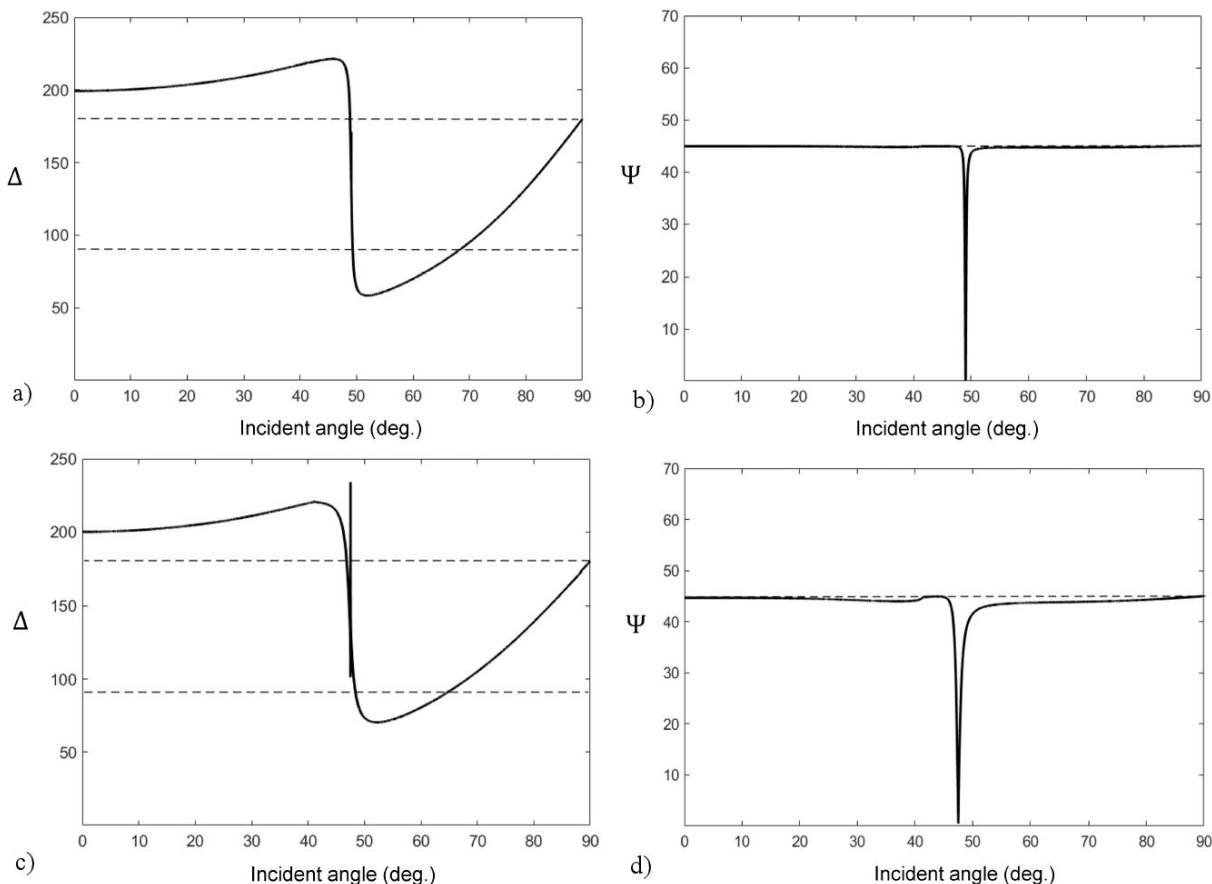


FIGURE 4. Multilayer SPR simulation curves at different thicknesses of ZrO₂ with analyte for the angle of incidence in phase dependence Δ and angle of incidence in amplitude dependence Ψ for Ag and Au. a) and b) Silver: BK7/ZrO₂(5 nm)/Ag(55.11 nm)/ZrO₂(196 nm)/analyte, c) and d) Gold: BK7/ZrO₂(5 nm)/Au(49.55 nm)/ZrO₂(186 nm)/analyte.

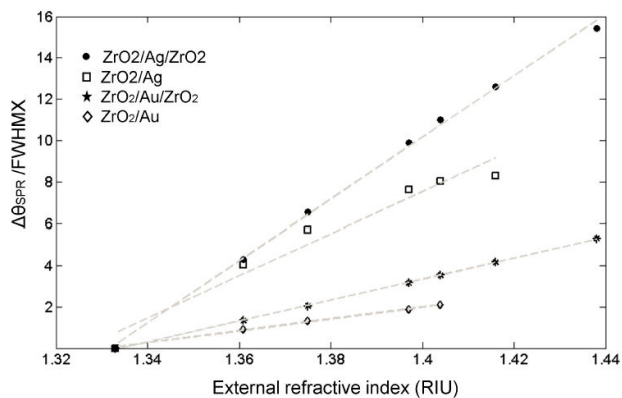


FIGURE 5. Change in the ratio $\Delta_{\theta_{SPR}}/FWHM$ with increasing refractive index of the dielectric medium: ZrO₂(5 nm)/Ag(55.11 nm) (squares), ZrO₂(5 nm)/Ag(55.11 nm)/ZrO₂(196 nm) (circles), ZrO₂(5 nm)/Au(49.55 nm) (diamonds) and ZrO₂(5 nm)/Au(49.55 nm)/ZrO₂(186 nm) (asterisk).

4. Conclusions

The multilayer SPR sensors ZrO₂/Ag/ZrO₂ and ZrO₂/Au/ZrO₂ were investigated theoretically. The effect

of the metal and dielectric layers on the optical properties of the film structure has been analysed and discussed. The thicknesses of Ag and Au metal layer with ZrO₂ film play an important role in the refractive index sensitivity and improve the SPR characteristics. The simulation work showed that the characterisation for the polarisation state of the DMDA multilayer reflected radiation under the polariton resonance condition presented remarkable behaviours that are classified in the complex plane of the ellipsometry equation. These behaviours are observed in the amplitude Ψ and phase Δ curves. For $\Delta = 0$ or π , the light that appears linearly polarised at any azimuth angle from the incident plane is linearly polarised after being reflected by DMDA, which would represent a polarised surface suppression analyser. Then if $\Delta = \pi/2$ or $3\pi/2$ the major or minor axes of the polarisation ellipse of the reflected light are linearly polarised for a certain azimuth angle and also aligned parallel or perpendicular to the plane of incidence. For $\tan \Psi = 1$, $R_p = R_s$ and $\rho = e^{i\Delta}$, the DMDA system acts as a reflection retarder. So, $\rho = \tan \Psi$ is a minimum or a maximum, these points indicate a given DMDA system that approximately behaves like a suppression polariser *s* or *p*. The results show that the FOM with the optimised ZrO₂ coating layer thicknesses for

Ag and Au were $0.196 \mu\text{m}$ and $0.186 \mu\text{m}$, respectively. The multilayer DMDA coating presented a minimum sensitivity of $50.619RIU^{-1}$ for $ZrO_2/Au/ZrO_2$ and the higher sensi-

tivity of $148.77RIU^{-1}$ for $ZrO_2/Ag/ZrO_2$ with promising features for SPR users to generalize this type of interfaces.

1. U. Arun *et al.*, Recent Advances in Optical Biosensors for Sensing Applications: a Review, *Plasmonics* **18** (2023) 735, <https://doi.org/10.1007/s11468-023-01803-2>.
2. Q. Wang *et al.*, Research advances on surface plasmon resonance biosensors, *Nanoscale* **14** (2022) 564, <https://doi.org/10.1039/D1NR05400G>.
3. P. Estrela *et al.*, *Optical biosensors, Essays Biochem.* **60** (2016) 91, <https://doi.org/10.1042/EBC20150010>.
4. V. Kodoyianni, Label-free analysis of biomolecular interactions using SPR imaging, *BioTechniques* **50** (2011) 32, <https://doi.org/10.2144/000113569>.
5. J. Cao *et al.*, Comparison of Surface Plasmon Resonance and Localized Surface Plasmon Resonance-based optical fibre sensors, *Journal of Physics: Conference Series* **307** (2011) 012050, <https://doi.org/10.1088/1742-6596/307/1/012050>.
6. C. M. and B. F., Theoretical Analysis of Multilayer Surface Plasmon Resonance Sensors Using Thin-Film Optical Admittance Formalism, *Plasmonics* **10** (2015) 1467, <https://doi.org/10.1007/s11468-015-9945-y>.
7. S. S. Gaur and A. P. Singh, Theoretical analysis and optimization of sensing parameters of surface plasmon resonance sensor, *Z NATURFORSCH A* **78** (2023) 89, <https://doi.org/10.1515/zna-2022-0128>.
8. S. Bao, H.-j. Li, and G.-g. Zheng, Concentration sensor with multilayer thin film-coupled surface plasmon resonance, *Optoelectron. Lett.* **17** (2021) 289, <https://doi.org/10.1007/s11801-021-0088-4>.
9. K. M. McPeak *et al.*, Plasmonic Films Can Easily Be Better: Rules and Recipes, *ACS Photonics* **2** (2015) 326, <https://doi.org/10.1021/ph5004237>.
10. D. L. Wood and K. Nassau, Refractive index of cubic zirconia stabilized with yttria, *Appl. Opt.* **21** (1982) 2978, <https://doi.org/10.1364/AO.21.002978>.
11. J. Dong *et al.*, Side-polished few-mode fiber based surface plasmon resonance biosensor, *Opt. Express* **27** (2019) 11348, <https://opg.optica.org/oe/abstract.cfm?URI=oe-27-8-11348>.
12. M. Born and E. Wolf, Principles of optics: electromagnetic theory of propagation, interference and diffraction of light (Cambridge University Press 7th expanded ed., 1999).
13. Y. Yuan, L. Ding, and Z. Guo, Numerical investigation for SPRbased optical fiber sensor, *Sens. Actuators B Chem.* **157** (2011) 240, <https://doi.org/10.1016/j.snb.2011.03.056>.
14. N. Podraza and G. Jellison, Ellipsometry, In J. C. Lindon, G. E. Tranter, and D. W. Koppenaal, eds., *Encyclopedia of Spectroscopy and Spectrometry* (Third Edition), pp. 482-489 (Academic Press, Oxford, 2014), <https://doi.org/10.1016/B978-0-12-409547-2.10991-6>.
15. P. Y. Kuryoz, L. V. Poperenko, and V. G. Kravets, Correlation between dielectric constants and enhancement of surface plasmon resonances for thin gold films, *Phys. Status Solidi A* **210** (2013) 2445, <https://doi.org/10.1002/pssa.201329272>.
16. Mukhtar, Wan Maisarah, Halim, Razman Mohd, and Hassan, Hazirah, Optimization of SPR signals: Monitoring the physical structures and refractive indices of prisms, *EPJ Web Conf.* **162** (2017) 01001, <https://doi.org/10.1051/epjconf/201716201001>.
17. L. J. Sherry *et al.*, Localized Surface Plasmon Resonance Spectroscopy of Single Silver Nanocubes, *Nano Lett.* **5** (2005) 2034, <https://doi.org/10.1021/nl0515753>.
18. A. Shalabney and I. Abdulhalim, Electromagnetic fields distribution in multilayer thin film structures and the origin of sensitivity enhancement in surface plasmon resonance sensors, *Sens. Actuator A Phys.* **159** (2010) 24, <https://doi.org/10.1016/j.sna.2010.02.005>.
19. C. Peng *et al.*, Optical Waveguide Refractive Index Sensor for Biochemical Sensing, *Appl. Sci.* **13** (2023) 3829, <https://doi.org/10.3390/app13063829>.